BMC Complementary Medicine and Therapies

RESEARCH Open Access

Quercetin parallels ascorbic acid in neuroprotection against manganese-induced toxicity in *Drosophila melanogaster*

Tolulope T. Arogundade[1*], Oluwasegun D. Olatomide[1], David A. Adeleye[1], Eberechi Nwoke[1], Vanessa C. Adim[1], Ayodele Omotefe[1], Adedamola A. Bayo-Olugbami[2], Dayo R. Omotoso[1] and Ismail Gbadamosi[3*]

Abstract

Quercetin (QCT) is a dietary flavonoid with reported antioxidant and neuroprotective properties, but direct comparisons with established antioxidants, such as ascorbic acid (AA), under chemically induced neurotoxic stress are limited. We compared Quercetin and AA in adult *D. melanogaster* using a manganese (Mn)-sensitized model to capture Parkinson-like motor and biochemical vulnerability. Treatment groups comprised: Control; Mn (15 mM); AA (10 mM); Quercetin 0.5 mM/3.0 mM; AA + Mn; Quercetin 0.5 mM/3.0 mM + Mn. Each vial represented an independent biological replicate (mixed sex); biochemical and genomic assays were performed using $n = 4$ vials/group. Outcomes included survival, locomotor performance (RING), redox endpoints (GSH/GSSG, H_2O_2, MDA, SOD, CAT), neuromodulators (AChE, dopamine), DNA fragmentation index (DFI), and advanced glycation end-products (AGEs). Omnibus tests (ANOVA or Kruskal-Wallis) were followed by Tukey HSD or Dunn-style pairwise comparisons; two pre-specified pooled contrasts were tested with Welch comparisons and effect sizes reported (mean differences, 95% CI, Cohen's d); pooled p-values were adjusted (Holm, BH). Quercetin and AA produced comparable protective effects, as both preserved climbing behaviour and partially restored the redox balance versus Mn. One Tukey-adjusted pairwise result reached significance (Control vs. quercetin low + Mn for DFI, p_adj = 0.049). A pooled contrast showed reduced H_2O_2 for Quercetin (Q_all vs. AA_all: mean diff = 0.498 µmol·g^{-1}, 95% CI 0.153–0.844; Welch t(13.27) = 3.11, $p = 0.0082$; d ≈ 1.38), but this and other pooled signals did not survive conservative family-wise correction across all pooled tests. In conclusion, although they are overall comparable, our data suggest that quercetin may have a superior, specific effect on reducing H_2O_2 and protecting DNA integrity (DFI). These endpoints are now prioritized for confirmatory studies.

Highlights

- Quercetin and ascorbic acid (vitamin C) produced comparable neuroprotective effects in manganese-sensitized *D. melanogaster*, preserving locomotor performance and attenuating oxidative stress.
- A pooled contrast indicated a considerable reduction in H_2O_2 and DFI with Quercetin compared to AA, suggesting that H_2O_2 and DFI might be prioritized endpoints.

*Correspondence:
Tolulope T. Arogundade
arogundadet@run.edu.ng
Ismail Gbadamosi
ismail.gbadamosi@port.lukasiewicz.gov.pl

Full list of author information is available at the end of the article

- Several endpoints (GSSG/GSH balance, AGEs) showed large effect sizes favouring quercetin in pooled contrasts. However, these signals did not survive conservative family-wise correction across the whole test family; therefore, the results are hypothesis-generating.

Keywords Quercetin, Ascorbic acid, Manganese, *Drosophila melanogaster*, Oxidative stress, DNA fragmentation

Graphical Abstract

Schematic overview of the experimental workflow testing quercetin (Q) and ascorbic acid (AA) in adult *Drosophila melanogaster* exposed to manganese (Mn). Eight treatment groups were studied (Control, Mn (15 mM), AA (10 mM), Q (0.5 mM), Q (3.0 mM), AA + Mn, Q (0.5 mM) + Mn, Q (3.0 mM) + Mn), with n = 4 independent vials per group (mixed-sex). Outcomes included survival, locomotor activity (RING assay), redox markers (GSH, GSSG, H_2O_2, MDA, SOD, and CAT), neuromodulators (AChE, dopamine), advanced glycation end-products (AGEs), and DNA fragmentation index (DFI). Statistical analyses combined omnibus and pairwise tests with pre-specified pooled contrasts (Q_only vs AA_only; Q_all vs AA_all). Results indicated that quercetin broadly paralleled AA in preserving motor performance and redox balance, with notable signals at H_2O_2 and DFI endpoints that warrant targeted confirmatory studies.

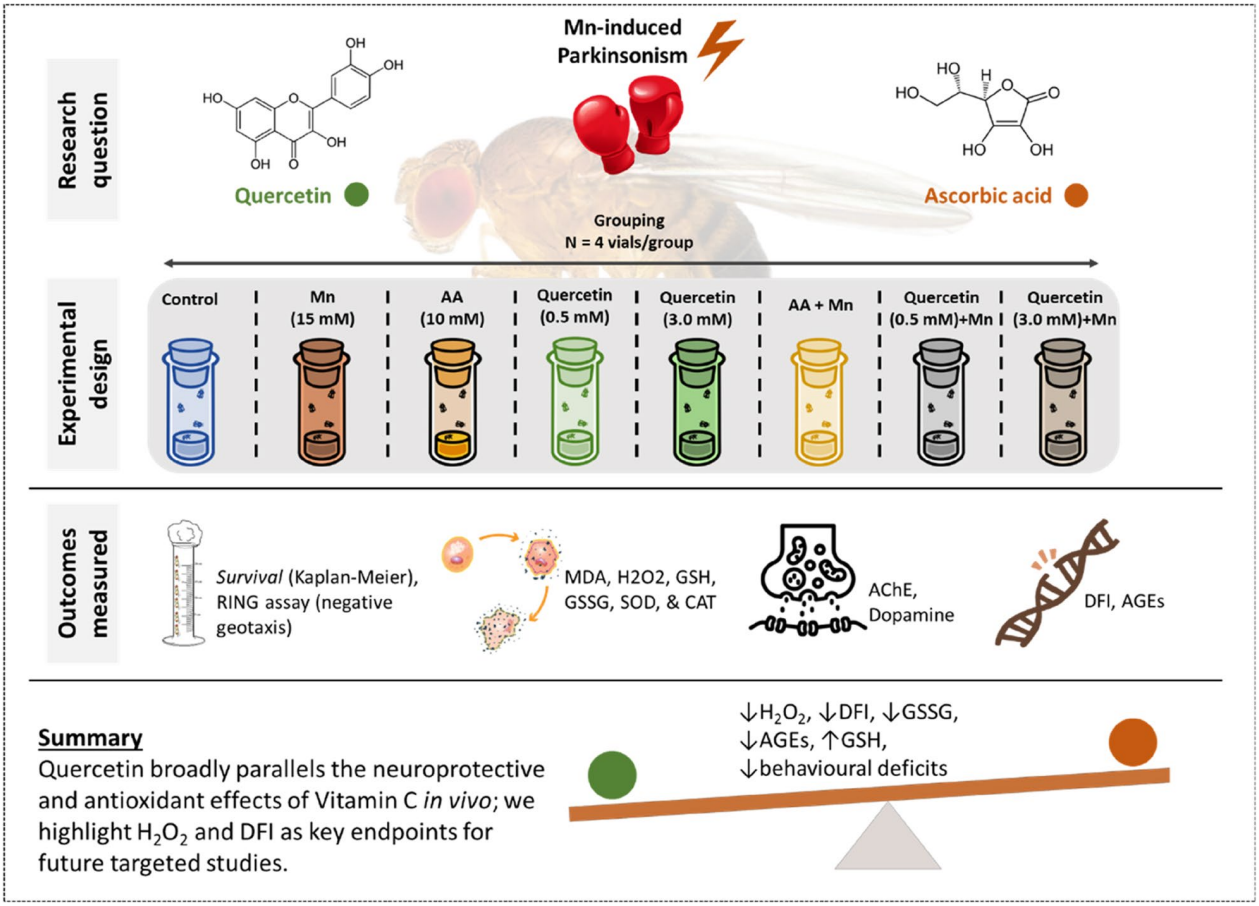

Introduction

Neurodegenerative disorders such as Parkinson's disease, Alzheimer's disease, and amyotrophic lateral sclerosis are growing in prevalence worldwide and now represent a significant and expanding burden on global health [1]. Their prevalence has increased steadily over the past three decades, with Parkinson's disease alone now affecting more than 11 million people globally [2]. These conditions are characterized by the gradual loss of vulnerable neuronal populations, and a substantial body of evidence suggests that oxidative stress, impaired redox homeostasis, mitochondrial dysfunction, and declining cellular resilience are central contributors to their pathogenesis [3].

Among environmental factors associated with neurodegeneration, chronic exposure to manganese has received considerable attention [4]. Manganese is an essential metal; however, elevated or prolonged exposure

in humans can produce key dyshomeostatic features observed across multiple neurodegenerative conditions, including locomotor impairment, dopaminergic dysfunction, mitochondrial impairment, and lysosomal dysregulation [5–10]. Clinical and epidemiological studies indicate that these neurological effects typically develop gradually, often emerging only after prolonged exposure to occupational or environmental factors [11, 12]. Human exposure to manganese is most common among welders, miners, ferroalloy workers, and individuals living in areas with contaminated dust or water. Epidemiological studies consistently report a higher prevalence of Parkinsonism and parkinsonian motor features in these occupational groups compared with the general population, reflecting the cumulative effects of chronic manganese inhalation and deposition in the brain [13, 14]. In such settings, manganese accumulation within the basal ganglia has been associated with oxidative injury, microglial activation, and progressive impairment of motor coordination [14]. Taken together, these epidemiological and mechanistic observations provide a clear rationale for using manganese-sensitized experimental models to investigate behavioural and biochemical markers of neurotoxicity and to evaluate candidate neuroprotective interventions.

Natural antioxidants and dietary polyphenols have gained prominence as candidate neuroprotective agents. Quercetin (QCT), a ubiquitous flavonoid found in fruits and vegetables, exerts antioxidant, anti-inflammatory, and mitochondrial-stabilizing effects across multiple in vivo and in vitro models [15, 16]. Ascorbic acid (vitamin C, AA), an essential water-soluble antioxidant, is routinely used as a reference compound in studies of redox modulation and neuroprotection [17, 18]. Comparing the antioxidant actions of QCT and AA within the same manganese-sensitized context provides a systematic approach to identifying which molecular features most effectively counteract neurotoxic oxidative stress. It may guide future strategies that explore their combined use. Despite this relevance, the literature provides almost no direct, side-by-side assessments of these compounds in a shared model. A unified evaluation is scientifically informative because QCT and AA are widely consumed, inexpensive, and mechanistically distinct antioxidants that engage different redox pathways. Examining their actions under identical conditions, therefore, allows a more straightforward interpretation of how accessible antioxidant molecules shape behavioural, biochemical, and genomic responses to manganese toxicity, and whether their protective effects converge or diverge under controlled oxidative stress.

To investigate these antioxidant effects under controlled neurotoxic conditions, we employed a simple, practical, and tractable model system using *Drosophila melanogaster*. This organism combines a well-defined nervous system with conserved oxidative and mitochondrial pathways, allowing rapid evaluation of behavioural and biochemical responses relevant to neurodegeneration. In this study, we utilized manganese (II) chloride ($MnCl_2$), a manganese salt commonly employed in *Drosophila* toxicology, to induce manganese-sensitized oxidative stress and motor deficits [10, 19, 20]. This paradigm is well established, with numerous studies demonstrating that dietary manganese chloride reliably induces locomotor impairment and oxidative injury in flies, serving as a suitable platform for evaluating candidate protective agents [21]. The model enables integrated assessment of locomotor function, redox balance, lipid peroxidation, and DNA integrity, including the DNA fragmentation index (DFI) [22, 23]. In addition, parallel measurements of acetylcholinesterase (AChE) activity and dopamine content provide complementary insight into neurotransmission pathways implicated in manganese-related neurotoxic stress [23].

Here, we compared QCT and AA in adult *D. melanogaster* exposed to control or manganese-containing diets. We evaluated a broad panel of outcomes encompassing locomotor behaviour, redox status, neuromodulatory markers, and indices of oxidative and genomic stress. Advanced glycation end-products (AGEs) are chemically diverse, relatively stable adducts formed through non-enzymatic "glycation/glycoxidation" reactions between reactive carbonyls (often derived from sugars) and biomolecules (proteins, lipids, or nucleic acids). AGEs can amplify oxidative stress and inflammation, in part through receptor-mediated signaling (e.g., RAGE), and have been implicated in aging and neurodegenerative processes [24, 25]. In *D. melanogaster*, AGEs accumulate with age and can be experimentally modulated, supporting their use as an informative glycoxidative-stress endpoint in this model [26]. The analytic design incorporated pre-specified pooled contrasts to improve the precision of QCT-versus-ascorbic-acid comparisons and to strengthen inference across related endpoints. By examining both antioxidants within the same manganese-sensitized framework, we aimed to characterize their relative capacities to modulate oxidative balance, behavioural performance, and molecular stress signatures in vivo. This integrative approach provides a structured basis for identifying endpoints most sensitive to antioxidant intervention and offers a platform for guiding future mechanistic and confirmatory studies in higher-order systems.

Materials & methods

Ethics statement

All experiments used *D. melanogaster* and therefore did not require approval from the institutional animal care committee [27]. Experiments followed best practices for

invertebrate research and reporting (ARRIVE-style handling and minimizing suffering).

D. Melanogaster strains and maintenance

Fly husbandry and experimental exposures were performed at the Department of Human Anatomy, Redeemer's University, Ede, Nigeria. Adult *D. melanogaster* (wild-type Oregon R) was used for all experiments. Flies were maintained under standard laboratory conditions (25 ± 1 °C, 60–70% relative humidity, 12 h light/dark cycle) on a basal diet recipe containing cornmeal, sucrose/glucose, Baker's yeast, agar, nipagin) as detailed by Abolaji et al. [28, 29]. Newly eclosed flies (a mixed-sex cohort of 1–3 days old) were used for all experiments. Each vial contained 10 flies with a fixed 1:1 sex ratio (5 females, 5 males) across all treatment conditions, so density and sex composition were held constant. We used mixed-sex cohorts to provide a general adult physiological readout; however, we acknowledge that mating can alter female physiology and oxidative-stress susceptibility and may therefore contribute additional variability in mixed-sex designs [30].

Experimental design and grouping

Flies were randomly allocated into eight groups with four independent biological replicates (one vial = one replicate; no pooling across vials). The groups were: Control (untreated), Manganese (Mn, 15 mM) exposure, AA (AA, 10 mM) only, QCT (low dose, 0.5 mM), QCT (high dose, 3.0 mM), AA + Mn, QCT (low dose) + Mn, and QCT (high dose) + Mn. Doses of Mn, QCT, and AA were selected based on previous literature and a survival analysis to reflect biologically relevant but non-lethal exposures [20, 21, 23, 31–36]. Treatments were incorporated into the food medium for 14 days.

Compound preparation

Quercetin (quercetin hydrate; Molychem, India [CAS No. 849061-97-8]) was prepared as a concentrated stock by dissolving the required mass in distilled water with gentle heating (≤ 40 °C) and vortexing for about 10 min. Stocks were diluted into molten fly food (cooled to ~ 50 °C) and mixed thoroughly to achieve final concentrations of 0.5 mM and 3.0 mM. Ascorbic acid (AA; Molychem, India [CAS No. 50-81-7]) was dissolved in distilled water and added to the medium to a final concentration of 10 mM. Manganese chloride tetrahydrate ($MnCl_2{\cdot}4\ H_2O$; Molychem, India [CAS No.13446-34-9]) was dissolved in distilled water and added to food to a final concentration of 15 mM. Media (5 mL per vial) were dispensed and allowed to solidify before transferring the flies. We visually inspected aliquots to verify complete dissolution and absence of precipitate; no precipitates were observed for the concentrations used.

Behavioural assay (RING)

Locomotor performance was assessed using the rapid iterative negative geotaxis (RING) assay, a validated measure of fly climbing ability. Groups of 10 flies (5 males and 5 females) were gently tapped to the bottom of a graduated vertical column, and climbing activity (number crossing the 8 cm mark) was video-recorded within a 10-second interval. The behavioural readout was based on both the number of flies that crossed the 8 cm mark and the resultant performance index [37–40].

Tissue collection and homogenization

At the end of the 14-day exposure period, flies were anaesthetized on ice (max 2 min) to minimize physiological perturbation. For each biological replicate, a single vial containing 10 flies (5 males, 5 females) was collected, and all flies were transferred into a chilled 1.5 mL microcentrifuge tube on ice. For biochemical assays, flies were homogenized manually on ice in 0.1 M phosphate-buffered saline (PBS, pH 7.4) at a ratio of 1:10 (w/v), corresponding to 10 flies in 1 mL of PBS. Homogenates were centrifuged (Eppendorf 5424) at 4,000 × g for 10 min at 4 °C, and the supernatants were aliquoted into pre-labelled tubes for immediate assay or frozen storage at -80 °C until processing. The total protein concentration in each supernatant was measured using the Bradford assay [47], with bovine serum albumin as a standard; these protein values were used to normalize all endpoints.

Oxidative stress assays

- Reduced glutathione (GSH) [41]: GSH Reduced glutathione (GSH) was measured as non-protein thiols (NPSHs). Briefly, aliquots of homogenate were protein-precipitated with 4% sulfosalicylic acid (SAS) (sample: SAS, 1:1 v/v), incubated at 4 °C for 60 min and centrifuged at 12,000 × g for 15 min at 4 °C. The resulting supernatant (containing non-protein thiols) was reacted with 5,5′-dithiobis(2-nitrobenzoic acid) (DTNB), and absorbance was measured at 412 nm. Values were interpolated from a GSH standard curve and normalized to total protein (reported as nmol $GSH{\cdot}mg^{-1}$ protein) [41].
- Catalase (CAT) [42]: Catalase activity was assayed by incubating the sample with a defined concentration of H_2O_2 substrate for precisely 2 min at room temperature; the reaction was stopped with a catalase stop buffer. Residual H_2O_2 was measured via horseradish peroxidase (HRP)-mediated oxidation of 3,3′,5,5′-tetramethylbenzidine (TMB) with absorbance read at 653 nm. Catalase activity was compared with a certified catalase standard curve and is reported as U per mg protein [42].

- Superoxide dismutase (SOD) [43]: SOD activity was determined based on the inhibition of adrenaline auto-oxidation. A 10 µL aliquot of sample supernatant was combined with 240 µL of 0.05 M carbonate buffer (pH 10.2) in a microplate. The reaction was initiated by adding 25 µL of freshly prepared 0.3 mM adrenaline. The increase in absorbance at 480 nm was recorded every 30 s for 150 s. One unit of SOD activity was defined as the amount of enzyme required to inhibit the rate of adrenaline auto-oxidation by 50%. Activity was normalized to total protein and expressed as units per milligram protein [43].
- Hydrogen peroxide (H_2O_2): H_2O_2 was quantified using the Velikova et al. method: samples were extracted with 5.0 mL of 0.1% (w/v) trichloroacetic acid (TCA) per vial homogenate and centrifuged at 12,000 × g for 15 min at 4 °C. Aliquots (0.5 mL) of the supernatant were mixed with 0.5 mL of 10 mM phosphate buffer (pH 7.0) and 1.0 mL of 1 M potassium iodide, and absorbance was measured at 390 nm. H_2O_2 content was calculated using the extinction coefficient 0.28 $\mu M^{-1} \cdot cm^{-1}$ and normalized to protein (reported as $nmol \cdot mg^{-1}$ protein) [44].
- Malondialdehyde (MDA; TBARS) [45]: Lipid peroxidation was assessed by measuring thiobarbituric acid reactive substances (TBARS). A 50 µL aliquot of supernatant was combined with 100 µL of 0.67% thiobarbituric acid (TBA) in a 1:2 volume ratio. The mixture was incubated in a boiling water bath at 95–100 °C for 15 min. After cooling, the samples were centrifuged at 10,000 × g for 5 min. The absorbance of the supernatant was measured at 532 nm in a microplate reader. Malondialdehyde (MDA) concentration was determined using a standard curve prepared from 1,1,3,3-tetraethoxypropane (TEP) and expressed as nanomoles (nmol) of MDA per milligram (mg) of protein [45].

Genomic and glycation assays

- DNA fragmentation index (DFI): DFI was assessed using a diphenylamine colorimetric assay adapted from Gercel-Taylor. Briefly, cell/tissue pellets were resuspended in 0.8 mL of 0.01 M PBS (pH 7.4) plus 0.7 mL of ice-cold lysis buffer (10 mM Tris-HCl, pH 8.0, 1 mM EDTA, 0.2% Triton X-100, 100 mM NaCl). Lysates were incubated on ice for 15 min and then centrifuged at 12,000 × g for 15 min at 4 °C to separate low-molecular-weight (fragmented) DNA (supernatant) from high-molecular-weight genomic DNA (pellet). The supernatant (~ 1.5 mL) and resuspended pellet were each treated with 1.5 mL 10% TCA, incubated for 10 min at room temperature, centrifuged (500 × g, 4 °C, 15 min), resuspended in 5% TCA, boiled for 15 min, cooled and centrifuged (300 × g, 4 °C, 15 min). Aliquots (0.5 mL) of the clarified supernatant were mixed with 1 mL diphenylamine reagent and incubated overnight at 30 °C prior to reading at 600 nm. Percentage DNA fragmentation = OD_{600}(supernatant) / [OD_{600}(supernatant) + OD_{600}(pellet)] × 100 [46].
- Advanced glycation end-products (AGEs): measured using MyBioSource ELISA (Cat. No. MBS021326). Samples were diluted such that ~ 50 µg of total protein was applied per well; assays were performed exactly according to the manufacturer's instructions. Results are reported as ng AGE per mL protein.

Neuromodulatory markers

- Acetylcholinesterase (AChE): measured using Elabscience AChE ELISA (Cat. No. E-EL-R0355). Sample dilution and protein per well were selected to fall within the kit's linear range (50 µg protein/well). Samples were assayed in duplicate and interpolated against the kit standard curve; results are presented as nanomoles of substrate hydrolyzed per minute per milligram of protein.
- Dopamine: measured using Elabscience Dopamine ELISA (Cat. No. E-EL-0046). Samples were deproteinized/diluted according to the kit instructions to ensure that values fall within the linear range. The assay employs a competitive binding format with antibody specificity for dopamine and minimal cross-reactivity, as per the manufacturer's validation data. All ELISA runs included blanks, negative controls, and duplicates for both standards and samples.

Statistical analysis

Data were analyzed using GraphPad Prism (version 9.5.0, GraphPad Software, San Diego, CA). Each vial of *D. Melanogaster* was treated as an independent biological replicate ($n = 4$ per group). All datasets were initially examined for distributional assumptions using the Shapiro-Wilk normality test and visual inspection of residual plots. When assumptions of normality were satisfied, differences among groups were assessed using one-way analysis of variance (ANOVA). Welch's ANOVA was employed for unequal variances. Post hoc multiple comparisons were conducted using Tukey's test. When normality was not satisfied, the nonparametric Kruskal-Wallis test was applied, followed by Dunn's post hoc test. In addition to omnibus tests, a priori contrasts were performed to compare pooled QCT-only groups (low and high dose) against AA-only or control groups. For

these comparisons, replicates were combined into new columns and analyzed using Welch's unpaired t-test, with effect sizes expressed as mean difference ± 95% confidence intervals. Cohen's *d* values were also calculated for parametric comparisons, while Cliff's delta was used for nonparametric contrasts. Data are presented as mean ± SEM or estimation plots for pre-specified contrasts. Statistical significance was set at $p < 0.05$, with effect size estimates and confidence intervals emphasized to aid interpretation, given the limited sample size.

Results

Survival and locomotor behaviour

Kaplan-Meier survival curves are shown in Fig. 1a. Mortality was primarily driven by manganese exposure; QCT alone did not produce acute toxicity at the tested doses. Negative geotaxis (RING) performance is summarized in Fig. 1c. Omnibus testing revealed between-group differences in climbing performance; post-hoc Tukey/Dunn pairwise tests indicated that QCT-treated groups maintained climbing ability comparable to that of AA-treated groups and superior to Mn alone.

Antioxidant enzymes, oxidative stress, and inflammatory markers

Figure 2 (a-f) displays group distributions for reduced glutathione (GSH), oxidized glutathione (GSSG), hydrogen peroxide (H_2O_2), malondialdehyde (MDA), superoxide dismutase (SOD) and catalase (CAT). For most redox endpoints, an omnibus test (ANOVA or Kruskal-Wallis, per endpoint) indicated between-group variance (see omnibus_anova_kruskal.csv in the Supplementary Materials). After Tukey or Dunn post-hoc adjustment, most pairwise comparisons among the eight groups were not statistically significant at $\alpha = 0.05$. In particular, direct pairwise comparisons between QCT and AA groups for the biochemical markers in Fig. 2 were generally non-significant after adjustment; however, several contrasts produced unadjusted $p < 0.05$ and large effect sizes, indicating consistent trends favouring QCT (lower H_2O_2, lower GSSG, improved GSH). These trends are visible in the raw data distributions (Fig. 2) and the estimation plots (Fig. 4). In short, pairwise post-hoc testing of these endpoints supports the assertion that QCT performs at least as well as AA across this panel; however,

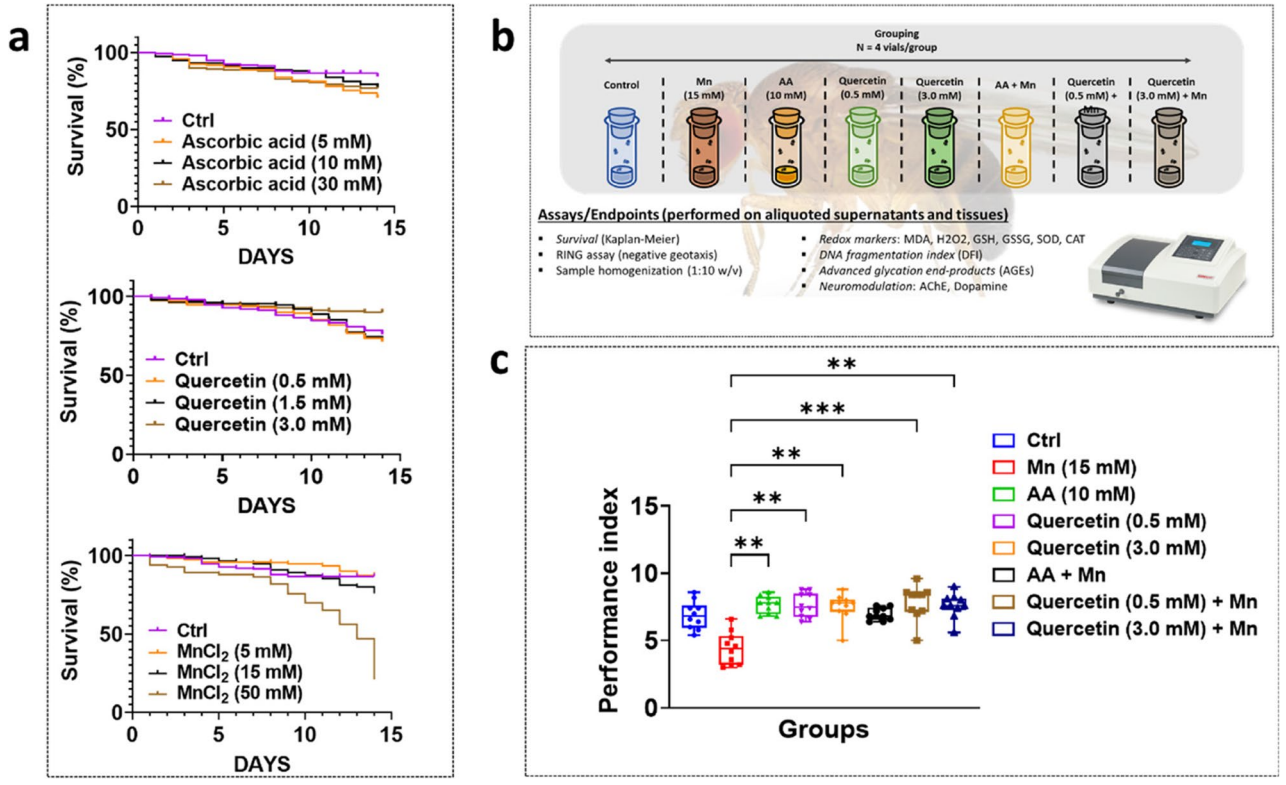

Fig. 1 Survival, experimental design, and locomotor performance. **a** Kaplan-Meier survival plots for flies receiving AA (AA; top), QCT (middle), and manganese (Mn; bottom). Curves show the proportion surviving over the exposure period. Survival differences were evaluated by the log-rank (Mantel-Cox) test. **b** Schematic of experimental groups and timeline. Eight treatment groups were used: Control (Ctrl), Mn (15 mM), AA (10 mM), QCT (0.5 mM), QCT (3 mM), AA + Mn, QCT 0.5 mM/3.0 mM + Mn; each vial = one independent biological replicate (mixed-sex, $n = 4$ vials per group for biochemical assays; see Methods). **c** Performance index from the RING (negative geotaxis) assay. Values are shown as individual vial points overlaid on box-and-whiskers plots (median, IQR; Tukey whiskers). Group differences were tested using the Kruskal-Wallis test with Dunn's multiple-comparisons post hoc test (Kruskal-Wallis test results reported on the panel). For all panels, * indicates $p < 0.05$, ** $p < 0.01$, *** $p < 0.001$

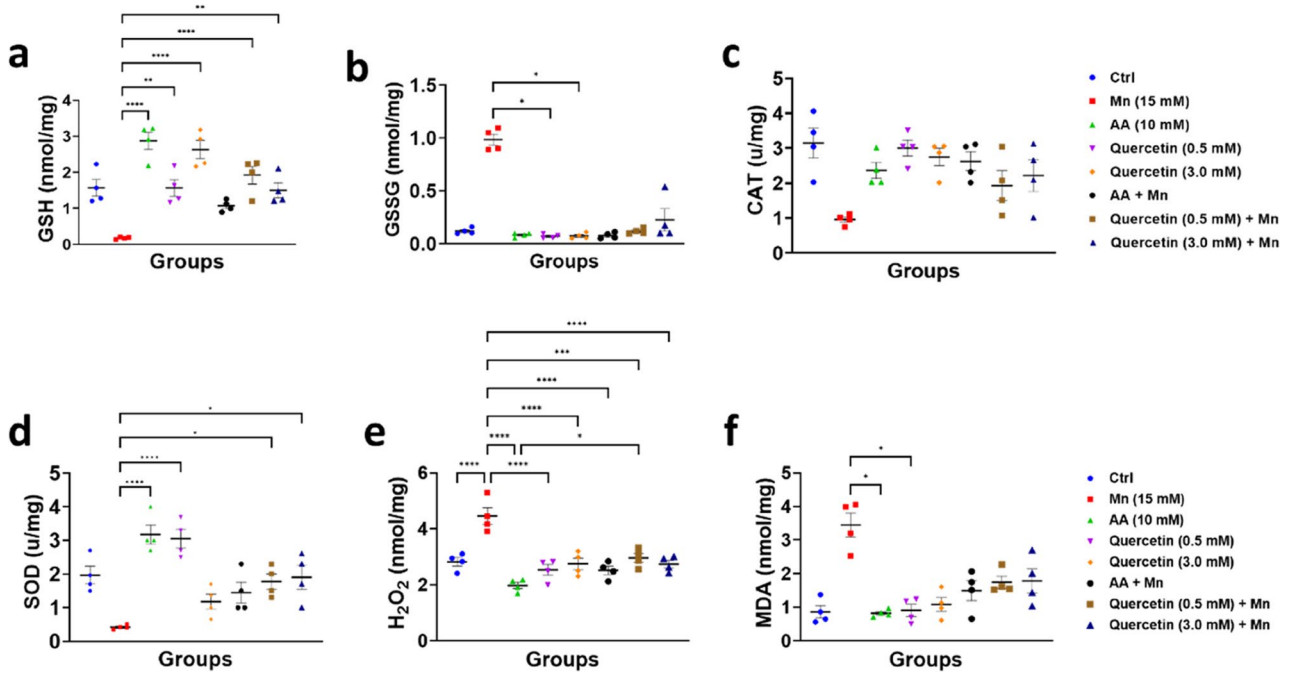

Fig. 2 Redox and inflammatory marker profiles across treatment groups. Panels show group-level distributions (individual vial datapoints) for: (**a**) reduced glutathione (GSH), (**b**) oxidized glutathione (GSSG), (**c**) catalase (CAT), (**d**) superoxide dismutase (SOD), (**e**) hydrogen peroxide (H_2O_2), and (**f**) malondialdehyde (MDA; lipid peroxidation). Statistical tests are noted per panel: one-way ANOVA (panels **a**, **d**, & **e**) or Kruskal-Wallis (panels **b**, **c**, **f**) according to distributional checks; post hoc pairwise comparisons were performed with Tukey's or Dunn's test as appropriate (see Methods). $n = 4$ independent vials per group. Asterisks indicate unadjusted significance levels on the figure (* $p < 0.05$; ** $p < 0.01$; *** $p < 0.001$)

the evidence is driven mainly by effect size rather than statistically conclusive pairwise comparisons.

Neuromodulatory and genomic endpoints

Figure 3 presents acetylcholinesterase (AChE), dopamine, DNA fragmentation index (DFI) and advanced glycation end-products (AGEs). Omnibus tests indicated modest group variance for neuromodulatory measures, but no pairwise Tukey/Dunn comparisons among QCT vs. AA groups reached adjusted significance; raw values and group means are shown in Fig. 3 (a & b). These data indicate no evidence of adverse neuromodulatory effects of QCT at the tested doses.

Similarly, omnibus testing showed between-group variance for DFI. Follow-up Tukey HSD identified one pairwise adjusted-significant comparison: Control vs. QCT (0.5 mM) + Mn, Tukey p_adj = 0.049 (Fig. 3c). This observation indicates that the group had reduced DNA fragmentation relative to the control under the specific pairwise test reported. Other pairwise comparisons of DFI (including direct QCT vs. AA pairs) were not statistically significant, although pooled contrasts (Fig. 4) indicate larger effect sizes favouring QCT. Pairwise post-hoc tests for AGEs returned no adjusted-significant QCT vs. AA differences (Fig. 3d); pooled contrasts produced large effect sizes in some comparisons (Fig. 4).

Pooled contrasts and estimation plots

Because many individual pairwise comparisons were underpowered given *the sample size per group, we evaluated pre-specified pooled contrasts to increase precision for the primary comparisons of interest, particularly* Q_only vs. AA_only and Q_all vs. AA_all. For each pooled contrast, we report the mean difference, 95% CI, Welch t-value and degrees of freedom (df), raw p-value, and Cohen's d; these are visualized as estimation plots in Fig. 4 and fully enumerated in the Supplementary file (pooled contrast.xls). Specific key pooled findings include:

- Hydrogen peroxide (Q_all vs. AA_all): Mean difference = 0.498 $\mu mol \cdot g^{-1}$ (95% CI 0.153 to 0.844), Welch t(df ≈ 13.27) = 3.11, $p = 0.0082$, Cohen's d ≈ 1.38 (Fig. 4). This pooled result indicates a considerable and precise reduction in HYDROGEN PEROXIDE associated with QCT pooling.
- DFI and AGEs: Pooled contrasts for DFI and AGEs showed large effect sizes favouring QCT (Cohen's d often > 0.8) and several raw pooled p-values < 0.05. For example, Q_only vs. Control for DFI: mean diff ≈ 16.5% (95% CI 3.39–29.6), raw $p \approx 0.021$, d ≈ 1.76.

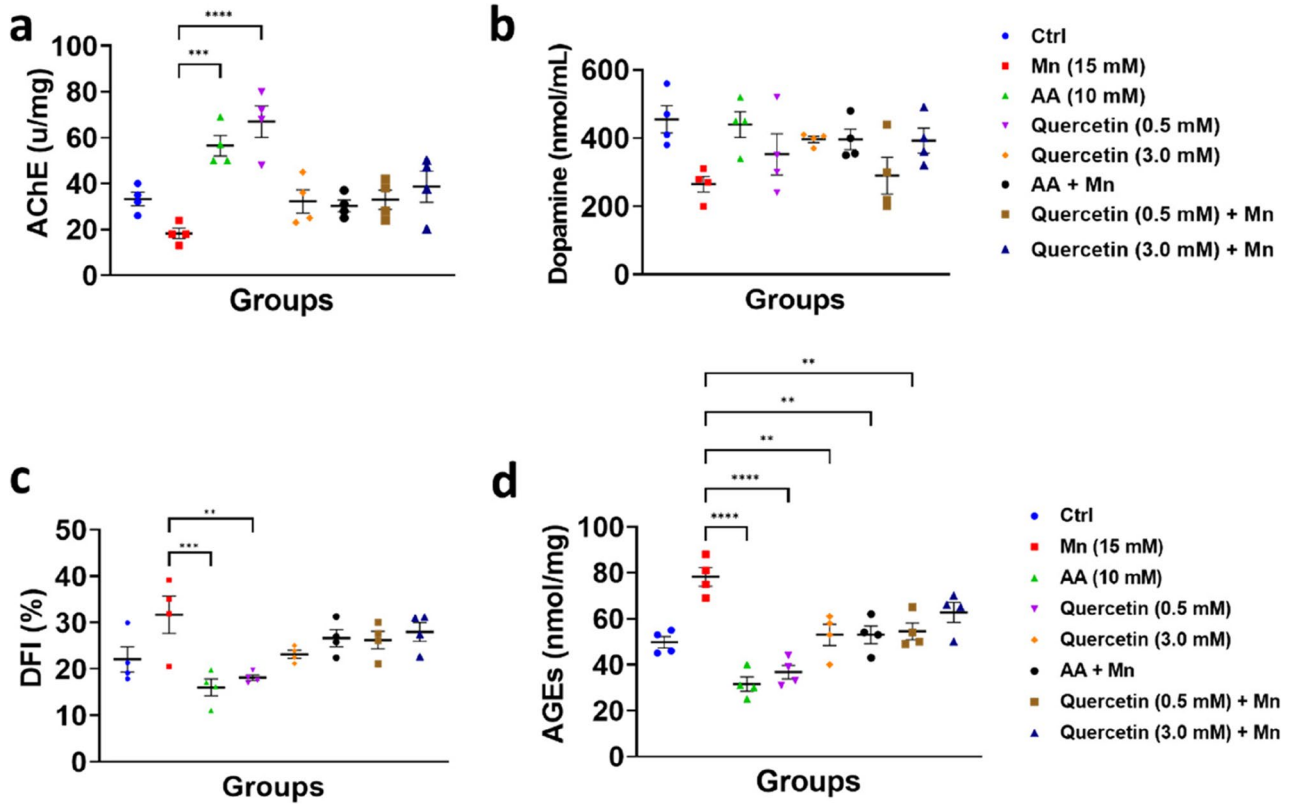

Fig. 3 Neuromodulatory markers and genomic damage. Top panels: (**a**) acetylcholinesterase (AChE) activity and (**b**) dopamine concentration, each plotted as individual vial datapoints. Bottom panels: (**c**) DNA fragmentation index (DFI, % fragmented DNA) and (**d**) advanced glycation end-products (AGEs, ng·mL^{-1} protein). Group comparisons were tested using one-way ANOVA or the Kruskal-Wallis test, as dictated by the normality of the data; post hoc tests were performed as described in the Methods section. $n = 4$ independent vials per group. Asterisks on panels denote unadjusted pairwise significance

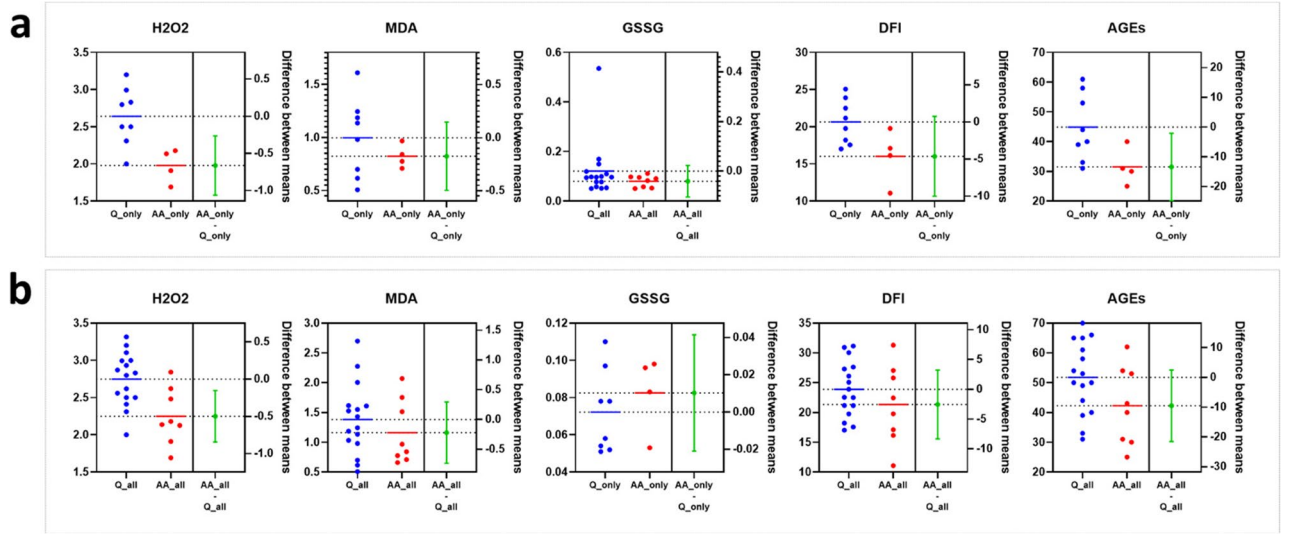

Fig. 4 Summary of pre-specified pooled contrasts (estimation plots) across selected endpoints. Panels present estimation plots for pooled contrasts (top panel, **a**: Q_only vs AA_only; bottom panel, **b**: Q_all vs AA_all) for the indicated biochemical/genomic endpoints (H_2O_2, MDA, GSSG, DFI, & AGEs). For each contrast, the left subpanel shows raw pooled data points (jittered) and the right subpanel shows the mean difference (comparator) with 95% CI obtained from Welch's t-test

Although multiple pooled contrasts had small raw p-values, none of the pooled-contrast p-values remained < 0.05 after conservative family-wise Holm adjustment across the complete pooled test family. Thus, the pooled contrasts provide strong effect-size signals that are hypothesis-generating rather than multiplicity-robust discoveries.

Discussion

Manganese neurotoxicity is a mechanistically complex process that likely involves multiple initiating events converging on cellular dysfunction. Experimental evidence suggests that mitochondrial impairment, dysregulated metal transport, astrocyte/glial dysfunction, and neuroinflammatory responses are important contributors, which in turn can increase reactive oxygen species (ROS) production and oxidative burden [5, 8, 9, 47]. In the present dataset, manganese exposure produced the expected pattern of behavioural impairment and redox disruption, while quercetin and ascorbic acid broadly preserved locomotor performance and shifted multiple oxidative-stress markers toward control-like values. Across the biochemical panel, the most consistent signal favouring quercetin appeared at hydrogen peroxide (H_2O_2) and DNA integrity (DFI), whereas other endpoints showed directionally similar but less conclusive patterns after multiplicity control. These findings are biologically compatible with literature linking manganese neurotoxicity to oxidative injury and with prior evidence that quercetin can modulate oxidative/inflammatory pathways (including Nrf2-related signaling in other systems), but our interpretation remains cautious because mechanistic mediators (e.g., mitochondrial function and antioxidant transcriptional activation) were not directly measured here.

Typically, AA mitigates toxicity primarily by acting as a reducing antioxidant that supports both cytosolic and mitochondrial redox systems. Ascorbate donates electrons to neutralize reactive oxygen species such as superoxide and hydrogen peroxide and regenerates oxidized antioxidants, including glutathione and vitamin E, thereby preserving membrane integrity [48]. It maintains iron in its ferric state, reducing the catalytic formation of hydroxyl radicals through Fenton-type chemistry, which becomes especially relevant in manganese-stressed environments where redox-active metals amplify oxidative injury [49]. AA also stabilizes mitochondrial respiration, preserves ATP-generating capacity, and contributes to dopamine synthesis by supporting tetrahydrobiopterin-dependent hydroxylase activity, a pathway that is susceptible to oxidative disruption [50, 51]. Although ascorbate can exhibit prooxidant behaviour in the presence of high concentrations of free transition metals, the biochemical pattern observed in our study, including reduced hydrogen peroxide, improved glutathione balance, and lower DNA fragmentation, indicates an overall antioxidant role under the dosing conditions used.

Building on the reducing antioxidant effects of AA, the distinct polyphenolic mechanisms of QCT provide an informative contrast for understanding how divergent antioxidant chemistries influence manganese-induced oxidative injury. QCT attenuates manganese neurotoxicity by acting at several points along the oxidative and mitochondrial injury cascade. As a polyphenolic flavonoid, QCT directly scavenges superoxide, hydrogen peroxide, and peroxyl radicals, and can chelate redox-active metals, thereby reducing their ability to catalyze ROS formation. QCT stabilizes mitochondrial membranes, preserves mitochondrial permeability, and reduces the opening of the permeability transition pore, thereby limiting manganese-induced collapse of mitochondrial potential [52, 53]. It also inhibits upstream ROS-generating enzymes, including xanthine oxidase and NADPH oxidase, and modulates apoptotic signalling through regulation of Bcl-2, Bax, and caspase pathways. A primary mechanism involves activation of Nrf2, which induces HO-1, NQO1, and the rate-limiting enzyme for glutathione synthesis, glutamate-cysteine ligase (GCL). In our dataset, quercetin was associated with lower H_2O_2 and a more favourable glutathione redox profile (measured GSH/GSSG endpoints), alongside reduced DNA fragmentation. Because we did not directly assess mitochondrial function (e.g., membrane potential, respiration/ATP production, or mitochondrial ROS), we do not interpret these results as demonstrating mitochondrial stabilization; rather, mitochondrial protection remains a plausible mechanism suggested by prior literature and should be tested directly in follow-up experiments.

Taken together, these mechanistic profiles show that QCT and AA counter manganese-induced oxidative injury through distinct yet convergent antioxidant strategies. Ascorbate primarily maintains reductive capacity, supports endogenous antioxidant recycling, and preserves mitochondrial and membrane stability. In contrast, QCT reinforces antioxidant defences by activating Nrf2-dependent pathways, stabilizing mitochondrial integrity, and limiting upstream ROS generation. Although these routes differ in their molecular entry points, they converge on key biochemical outcomes in our model, including improved glutathione balance, reduced hydrogen peroxide, and lower DNA fragmentation. This integrated perspective provides a coherent explanation for the broadly comparable protective profiles observed in the manganese-sensitized fly model. Moreover, it underscores the value of examining chemically and mechanistically distinct antioxidants within a unified experimental framework, as such comparisons may reveal complementary modes of action that could

inform future combinatorial or translational antioxidant strategies in manganese-related neurotoxicity.

The biochemical pattern observed in our study aligns well with this mechanistic interpretation. QCT's association with lower hydrogen peroxide and a more favourable GSH/GSSG balance fits its established radical-scavenging and redox-modulating properties [15, 16, 18]. Because hydrogen peroxide is a central ROS species capable of driving oxidative DNA lesions such as 8-oxo-dG and lipid peroxidation, its reduction offers a plausible upstream explanation for the decreased DNA fragmentation (DFI) we observed. The AChE and dopamine data further show no evidence of neuromodulatory toxicity at the doses used, providing functional context for the preserved locomotor behaviour. Taken together, reduced hydrogen peroxide and strengthened glutathione balance plausibly underpin the behavioural protection observed in the RING assay [54–57].

Drosophila-specific evidence supports the biological relevance of both compounds in this model. Although flies cannot synthesize ascorbate de novo, dietary vitamin C accumulates in their tissues and influences oxidative balance, lifespan, and stress resilience [58, 59]. More recent work shows that ascorbate enhances survival during oxidative challenge and reduces lipid peroxidation and thiol oxidation [32, 60–62]. These results are particularly relevant in manganese-sensitized states, where exogenous reducing capacity helps compensate for mitochondrial ROS overload. Similarly, quercetin is bioactive in insects: flies absorb dietary quercetin, convert it to conjugated metabolites with preserved antioxidant activity, and exhibit reduced ROS generation, preserved thiol pools, and reduced genotoxicity following exposure [63, 64]. These insect-specific data support the use of AA and QCT as biologically meaningful comparators in models of manganese-induced oxidative stress.

Critically, the statistical interpretation of our findings reinforces the biological perspective above. Conventional pairwise comparisons revealed few adjusted significant differences across treatment groups, reflecting modest sample sizes and multiple testing. The estimation-focused pooled-contrast analysis increased precision and revealed large effect sizes for hydrogen peroxide and DNA fragmentation. Although these signals did not persist after conservative family-wise adjustment, the pooled-contrast and pairwise perspectives together support a cautious but internally consistent conclusion: Quercetin and ascorbic acid exhibit broadly parallel protective effects against manganese-induced oxidative and behavioural dysfunction, while highlighting hydrogen peroxide and DFI as priority endpoints for follow-up work.

Manganese exposure models produce Parkinson-like motor deficits and dopaminergic dysregulation. While manganism is not identical to idiopathic Parkinson's disease (PD), it is a well-established sensitizer for nigrostriatal dysfunction in experimental systems [5, 6, 9, 10, 65, 66]. Demonstrating that a dietary flavonoid (QCT) produces effect-size comparable protection to vitamin C across behaviour, redox, and genomic endpoints in this context identifies measurable in-vivo endpoints (Hydrogen Peroxide, DFI) that can be prioritized in translational pipelines (e.g., dose-response, pharmacokinetics, mammalian replication). To increase translational relevance, future work should explicitly relate exposure levels to dietary equivalents or achievable pharmacological concentrations and test whether protective signals persist in mammalian PD models or in neuronal cell systems that more directly model human dopaminergic vulnerability [7, 23, 40]. Measurement of dopamine content (and AChE activity as a cholinergic readout) provides functional context: dopaminergic decline is central to PD motor phenotypes. At the same time, cholinergic dysfunction also contributes to the non-motor and cognitive components of neurodegeneration; our results, therefore, link biochemical protection with preserved behaviour in a Mn-sensitized model [9].

From a nutritional and complementary-medicine perspective, the finding that quercetin performs comparably to ascorbic acid in this model is noteworthy. Quercetin is abundant in common plant-derived foods such as onions, apples, berries, and capers, making it accessible as a dietary antioxidant. While direct translational conclusions must be cautious, our results support the rationale behind diverse, polyphenol-rich diets and justify further exploration of quercetin's bioavailability and brain penetration relative to the well-characterized pharmacokinetics of ascorbic acid.

Notably, several limitations temper the strength of the conclusions of this study. First, sample sizes per group were modest, which reduces statistical power for multiple comparisons and produces wider confidence intervals around effect estimates. Second, we used only a single concentration of each of the following: manganese, quercetin, and ascorbic acid. This limits interpretation, as dose-related relationships, thresholds, and potential biphasic effects could not be evaluated. Third, although the biochemical panel included key redox and neuromodulatory markers, the study did not incorporate mechanistic assays that directly link changes in hydrogen peroxide or DNA fragmentation to specific molecular events. Examples include quantitative measurement of 8-oxo-dG, analysis of Nrf2 or HO1 expression, or histological assessment of dopaminergic neuron integrity. Fourth, the manganese paradigm captures Parkinson-like vulnerability but does not reproduce the full spectrum of idiopathic Parkinson's disease. Finally, mixed-sex cohorts were used, which may have introduced sex-related

variability that was not formally assessed [9, 66–68]. For these reasons, extrapolation to human pathology requires caution. A further limitation is the use of mixed-sex cohorts without sex-stratified analyses. In *D. melanogaster*, mating and post-mating physiology can influence metabolism and oxidative-stress-related traits, and mating typically occurs within hours to the first day after eclosion under standard culture conditions. Although sex ratio and density were identical across our treatment groups, we cannot exclude treatment-specific effects on reproductive behaviour or reproductive physiology that could influence some measured endpoints [30, 69]. Also, future studies will therefore replicate key endpoints in male-only and female-only cohorts and/or in strictly virgin females collected within established virgin windows. Future mechanistic work will directly test antioxidant transcriptional responses in the fly, including the Keap1/Nrf2 pathway (CncC in *D. melanogaster*), which is activated by oxidants and regulates detoxification/antioxidant defenses in vivo. Candidate approaches include quantifying CncC/Nrf2 target-gene induction by qPCR and/or using available reporter lines to measure pathway activation under Mn ± antioxidant exposure.

Conclusion

This study provides a structured comparison of quercetin and ascorbic acid within a manganese-sensitized *D. melanogaster* model of oxidative and motor dysfunction. Both antioxidants produced broadly similar protective patterns across behavioural, redox, and genomic measures, with reductions in hydrogen peroxide and DNA fragmentation emerging as the most consistent and informative endpoints. These observations support a conservative interpretation, in which quercetin performs comparably to ascorbic acid under the tested conditions. The identification of hydrogen peroxide and DFI as sensitive readouts offers a clear foundation for future confirmatory work. Replication with expanded dose ranges, additional mechanistic assays, and complementary model systems will be necessary to determine the robustness and biological relevance of these antioxidant effects, as well as to clarify their potential value in manganese-related neurotoxicity research.

Abbreviations

AA	Ascorbic acid (vitamin C)
AGEs	Advanced glycation end-products
AChE	Acetylcholinesterase
ANOVA	Analysis of variance
CAT	Catalase
CI	Confidence interval
DF	Degrees of freedom
DFI	DNA fragmentation index
GSH	Reduced glutathione
GSSG	Oxidized glutathione
H_2O_2	Hydrogen peroxide
MDA	Malondialdehyde (lipid-peroxidation marker)
Mn ($MnCl_2$)	Manganese
N	Sample size (number of independent biological replicates/vials)
n.s.	Not significant
PD	Parkinson's disease
Q	Quercetin (use Q_only, Q_all as defined below)
Q_all	Pooled quercetin groups
Q_only	Pooled quercetin groups without Mn
RING	Rapid Iterative Negative Geotaxis (negative geotaxis/climbing assay)
SD	Standard deviation
SEM	Standard error of the mean
SOD	Superoxide dismutase

Supplementary Information

The online version contains supplementary material available at https://doi.org/10.1186/s12906-026-05378-3.

Supplementary Material 1.

Supplementary Material 2.

Supplementary Material 3.

Authors' contributions

Conceptualization: TTA; Methodology: TTA and ODO; Investigation: DAA, EN, VCA, and AO; Resources: DAA, EN, VCA, AO, and AAB; Visualisation: TTA; Formal Analysis: TTA, ODO, and IG; Writing (Original Draft): TTA; Writing (Review and Editing): TTA, ODO, AAB, DRO, and IG; Supervision: TTA, ODO, IG, and DRO. All authors have read and agreed to the final version of the manuscript.

Funding

This research received no specific grant from funding agencies in the public, commercial, or not-for-profit sectors.

Data availability

The data are available from the corresponding author upon reasonable request. However, the analysis results are contained in the supplementary information files.

Declarations

Ethics approval and consent to participate

Not applicable. All experiments used *D. melanogaster* (invertebrates) and therefore did not require approval from the Institutional Animal Care Committee.

Consent for publication

Not applicable.

Competing interests

The authors declare no competing interests.

Author details

[1]Department of Human Anatomy, Faculty of Basic Medical Sciences, Redeemer's University, Ede, Nigeria
[2]Department of Physiology, Faculty of Basic Medical Sciences, Osun State University, Osogbo, Nigeria
[3]Research Network Łukasiewicz – PORT Polish Centre for Technology Development, Wroclaw, Poland

Received: 2 October 2025 / Accepted: 8 April 2026
Published online: 15 April 2026

References

1. Gadhave DG, Sugandhi VV, Jha SK, Nangare SN, Gupta G, Singh SK, et al. Neurodegenerative disorders: Mechanisms of degeneration and therapeutic

approaches with their clinical relevance. Ageing Res Rev. 2024;99:102357. https://doi.org/10.1016/J.ARR.2024.102357.
2. Li M, Ye X, Huang Z, Ye L, Chen C. Global burden of Parkinson's disease from 1990 to 2021: a population-based study. BMJ Open. 2025;15:e095610. https://doi.org/10.1136/BMJOPEN-2024-095610.
3. Glass CK, Saijo K, Winner B, Marchetto MC, Gage FH. Mechanisms Underlying Inflammation in Neurodegeneration. Cell. 2010;140:918–34. https://doi.org/10.1016/j.cell.2010.02.016.
4. Mezzaroba L, Alfieri DF, Colado Simão AN, Vissoci Reiche EM. The role of zinc, copper, manganese and iron in neurodegenerative diseases. Neurotoxicology. 2019;74:230–41. https://doi.org/10.1016/J.NEURO.2019.07.007.
5. Morcillo P, Cordero H, Ijomone OM, Ayodele A, Bornhorst J, Gunther L, et al. Defective Mitochondrial Dynamics Underlie Manganese-Induced Neurotoxicity. Mol Neurobiol. 2021;58:3270–89. https://doi.org/10.1007/s12035-021-02341-w.
6. Milatovic D, Zaja-Milatovic S, Gupta RC, Yu Y, Aschner M. Oxidative damage and neurodegeneration in manganese-induced neurotoxicity. Toxicol Appl Pharmacol. 2009. https://doi.org/10.1016/j.taap.2009.07.004.
7. Dusek P, Roos PM, Litwin T, Schneider SA, Flaten TP, Aaseth J. The neurotoxicity of iron, copper and manganese in Parkinson's and Wilson's diseases. J Trace Elem Med Biol. 2015. https://doi.org/10.1016/j.jtemb.2014.05.007.
8. Oikawa S, Hirosawa I, Tada-Oikawa S, Furukawa A, Nishiura K, Kawanishi S. Mechanism for manganese enhancement of dopamine-induced oxidative DNA damage and neuronal cell death. Free Radic Biol Med. 2006;41:748–56. https://doi.org/10.1016/j.freeradbiomed.2006.05.018.
9. Harischandra DS, Ghaisas S, Zenitsky G, Jin H, Kanthasamy A, Anantharam V, et al. Manganese-induced neurotoxicity: new insights into the triad of protein misfolding, mitochondrial impairment, and neuroinflammation. Front Neurosci. 2019;13. https://doi.org/10.3389/fnins.2019.00654.
10. Altenhofen S, Wiprich MT, Nery LR, Leite CE, Vianna MRMR, Bonan CD. Manganese(II) chloride alters behavioral and neurochemical parameters in larvae and adult zebrafish. Aquat Toxicol. 2017;182:172–83. https://doi.org/10.1016/j.aquatox.2016.11.013.
11. Martins AC, Gubert P, Villas Boas GR, Meirelles Paes M, Santamaría A, Lee E, et al. Manganese Induced neurodegenerative diseases and possible therapeutic approaches. Expert Rev Neurother. 2020;20:1109. https://doi.org/10.1080/14737175.2020.1807330.
12. Mogi M. Manganese exposure is a risk for brain atrophy. Hypertension Research 2023 46:8. 2023;46:1883–5. https://doi.org/10.1038/s41440-023-01339-2.
13. Kulshreshtha D, Ganguly J, Jog M. Manganese and Movement Disorders: A Review. J Mov Disord. 2021;14:93–102. https://doi.org/10.14802/JMD.20123.
14. Lucchini RG, Aschner M, Yangho kim, Šarić M. Manganese. Handbook on the Toxicology of Metals. 2015;:975–1011. https://doi.org/10.1016/B978-0-444-59453-2.00045-7.
15. Costa C LG, Garrick JM, Roquè PJ, Pellacani. Mechanisms of neuroprotection by quercetin: counteracting oxidative stress and more. Oxid Med Cell Longev. 2016;2016. https://doi.org/10.1155/2016/2986796.
16. Chiang M-C, Tsai T-Y, Wang C-J. The Potential Benefits of Quercetin for Brain Health: A Review of Anti-Inflammatory and Neuroprotective Mechanisms. Int J Mol Sci. 2023;24:6328. https://doi.org/10.3390/ijms24076328.
17. Chang BJ, Jang BJ, Son TG, Cho IH, Quan FS, Choe NH, et al. Ascorbic acid ameliorates oxidative damage induced by maternal low-level lead exposure in the hippocampus of rat pups during gestation and lactation. Food Chem Toxicol. 2012. https://doi.org/10.1016/j.fct.2011.09.043.
18. Olajide OJ, Yawson EO, Gbadamosi IT, Arogundade TT, Lambe E, Obasi K, et al. Ascorbic acid ameliorates behavioural deficits and neuropathological alterations in rat model of Alzheimer's disease. Environ Toxicol Pharmacol. 2017;50. https://doi.org/10.1016/j.etap.2017.02.010.
19. Bonilla E, Contreras R, Medina-Leendertz S, Mora M, Villalobos V, Paz M, et al. Manganese toxicity in Drosophila melanogaster: Extension of the life span by resveratrol. Toxicol Environ Chem. 2012;94:742–7. https://doi.org/10.1080/02772248.2012.668787. ;REQUESTEDJOURNAL:JOURNAL:GTEC20;ISSUE:ISSUE:DOI.
20. Volpe RP, Sen A, Sharma A, Kathiresan V, Hoffman BM, Cox RT. Prophylactically Feeding Manganese to Drosophila Confers Sex-Specific Protection from Acute Ionizing Radiation Independent of MnSOD2 Levels. Antioxidants. 2025;14:134. https://doi.org/10.3390/antiox14020134.
21. Silva NC, Poetini MR, Bianchini MC, Almeida FP, Dahle MMM, Araujo SM, et al. Protective effect of gamma-oryzanol against manganese-induced toxicity in Drosophila melanogaster. Environ Sci Pollut Res. 2021;28:17519–31. https://doi.org/10.1007/s11356-020-11848-z.
22. Santarelli S, Londero C, Soldano A, Candelaresi C, Todeschini L, Vernizzi L, et al. Drosophila melanogaster as a model to study autophagy in neurodegenerative diseases induced by proteinopathies. Front Neurosci. 2023;17. https://doi.org/10.3389/fnins.2023.1082047.
23. Bonilla-Ramirez L, Jimenez-Del-Rio M, Velez-Pardo C. Acute and chronic metal exposure impairs locomotion activity in Drosophila melanogaster: a model to study Parkinsonism. Biometals. 2011;24:1045–57. https://doi.org/10.1007/s10534-011-9463-0.
24. Drenth H, Zuidema S, Bunt S, Bautmans I, van der Schans C, Hobbelen H. The Contribution of Advanced Glycation End product (AGE) accumulation to the decline in motor function. Eur Rev Aging Phys Activity. 2016;13:3. https://doi.org/10.1186/s11556-016-0163-1.
25. Ramasamy R, Vannucci SJ, Yan SS, Du, Herold K, Yan SF, Schmidt AM. Advanced glycation end products and RAGE: a common thread in aging, diabetes, neurodegeneration, and inflammation. Glycobiology. 2005;15:R16–28. https://doi.org/10.1093/glycob/cwi053. R.
26. Oudes AJ, Herr CM, Olsen Y, Fleming JE. Age-dependent accumulation of advanced glycation end-products in adult Drosophila melanogaster. Mech Ageing Dev. 1998;100:221–9. https://doi.org/10.1016/S0047-6374(97)00146-2.
27. Baenas N, Wagner AE. Drosophila melanogaster as an alternative model organism in nutrigenomics. Genes Nutr. 2019;14:14. https://doi.org/10.1186/s12263-019-0641-y.
28. Abolaji AO, Olaiya CO, Oluwadahunsi OJ, Farombi EO. Dietary consumption of monosodium L-glutamate induces adaptive response and reduction in the life span of < scp> *Drosophila melanogaster*. Cell Biochem Funct. 2017;35:164–70. https://doi.org/10.1002/cbf.3259.
29. Abolaji AO, Fasae KD, Iwezor CE, Aschner M, Farombi EO. Curcumin attenuates copper-induced oxidative stress and neurotoxicity in Drosophila melanogaster. Toxicol Rep. 2020;7:261–8. https://doi.org/10.1016/j.toxrep.2020.01.015.
30. Rush B, Sandver S, Bruer J, Roche R, Wells M, Giebultowicz J. Mating increases starvation resistance and decreases oxidative stress resistance in *Drosophila melanogaster* females. Aging Cell. 2007;6:723–6. https://doi.org/10.1111/j.1474-9726.2007.00322.x.
31. Kong Y, Li K, Fu T, Wan C, Zhang D, Song H, et al. Quercetin ameliorates Aβ toxicity in Drosophila AD model by modulating cell cycle-related protein expression. Oncotarget. 2016;7:67716–31. https://doi.org/10.18632/oncotarget.11963.
32. Sadiq IZ, Katsayal BS, Abdulazeez R, Omengwu YF, Adedoyin OS, Usman AG. Ascorbic acid increases survival rate and decreases oxidative stress via possible interaction with Nrf2-Keap1 in Drosophila melanogaster. Proceedings of the National Academy of Sciences, India Section B: Biological Sciences. 2025. https://doi.org/10.1007/s40011-025-01683-y.
33. Fragiorge EJ, Spanó MA, Antunes LMG. Modulatory effects of the antioxidant ascorbic acid on the direct genotoxicity of doxorubicin in somatic cells of Drosophila melanogaster. Genet Mol Biol. 2007;30:449–55. https://doi.org/10.1590/S1415-47572007000300025.
34. Deshpande C, Dhir A, Kulkarni SK. Antagonistic Activity of Ascorbic Acid (Vitamin C) on Dopaminergic Modulation: Apomorphine-Induced Stereotypic Behavior in Mice. Pharmacology. 2006;77:38–45. https://doi.org/10.1159/000092409.
35. Ternes APL, Zemolin AP, da Cruz LC, da Silva GF, Saidelles APF, de Paula MT, et al. Drosophila melanogaster - an embryonic model for studying behavioral and biochemical effects of manganese exposure. EXCLI J. 2014;13:1239–53.
36. Adedara IA, Abolaji AO, Rocha JBT, Farombi EO. Diphenyl Diselenide Protects Against Mortality, Locomotor Deficits and Oxidative Stress in Drosophila melanogaster Model of Manganese-Induced Neurotoxicity. Neurochem Res. 2016;41:1430–8. https://doi.org/10.1007/s11064-016-1852-x.
37. Liu C, Haynes PR, Donelson NC, Aharon S, Griffith LC. Sleep in Populations of *Drosophila Melanogaster*. eNeuro. 2015;2. https://doi.org/10.1523/ENEURO.0071-15.2015. ENEURO.0071-15.2015.
38. Dilliane CC, Suelen F, Jaqueline V, Welligton LB. Valeriana officinalis and melatonin: Evaluation of the effects in Drosophila melanogaster rapid iterative negative geotaxis (RING) test. J Med Plants Res. 2017;11:703–12. https://doi.org/10.5897/JMPR2017.6492.
39. Friggi-Grelin F, Coulom H, Meller M, Gomez D, Hirsh J, Birman S. Targeted gene expression in *Drosophila* dopaminergic cells using regulatory sequences from tyrosine hydroxylase. J Neurobiol. 2003;54:618–27. https://doi.org/10.1002/neu.10185.

40. Coulom H, Birman S. Chronic Exposure to Rotenone Models Sporadic Parkinson's Disease in *Drosophila melanogaster*. J Neurosci. 2004;24:10993–8. https://doi.org/10.1523/JNEUROSCI.2993-04.2004.
41. Jollow DJ, Mitchell JR, Zampaglione N, Gillette JR. Bromobenzene-Induced Liver Necrosis. Protective Role of Glutathione and Evidence for 3,4-Bromobenzene Oxide as the Hepatotoxic Metabolite. Pharmacology. 1974;11:151–69. https://doi.org/10.1159/000136485.
42. Sinha AK. Colorimetric assay of catalase. Anal Biochem. 1972;47:389–94. https://doi.org/10.1016/0003-2697(72)90132-7.
43. Roth EF, Gilbert HS. The pyrogallol assay for superoxide dismutase: Absence of a glutathione artifact. Anal Biochem. 1984;137:50–3. https://doi.org/10.1016/0003-2697(84)90344-0.
44. Velikova V, Yordanov I, Edreva A. Oxidative stress and some antioxidant systems in acid rain-treated bean plants. Plant Sci. 2000;151:59–66. https://doi.org/10.1016/S0168-9452(99)00197-1.
45. Ohkawa H, Ohishi N, Yagi K. Assay for lipid peroxides in animal tissues by thiobarbituric acid reaction. Anal Biochem. 1979;95:351–8. https://doi.org/10.1016/0003-2697(79)90738-3.
46. Gercel-Taylor C. Diphenylamine assay of DNA fragmentation for chemosensitivity testing. In: Chemosensitivity. New Jersey: Humana Press. 2005:079–82. https://doi.org/10.1385/1-59259-889-7:079.
47. Carmona A, Roudeau S, Ortega R. Molecular Mechanisms of Environmental Metal Neurotoxicity: A Focus on the Interactions of Metals with Synapse Structure and Function. Toxics. 2021;9:198. https://doi.org/10.3390/toxics9090198.
48. Gęgotek A, Skrzydlewska E. Antioxidative and Anti-Inflammatory Activity of Ascorbic Acid. Antioxidants. 2022;11:1993. https://doi.org/10.3390/ANTIOX11101993.
49. Shen J, Griffiths PT, Campbell SJ, Utinger B, Kalberer M, Paulson SE. Ascorbate oxidation by iron, copper and reactive oxygen species: review, model development, and derivation of key rate constants. Sci Rep 2021. 2021;11:1. https://doi.org/10.1038/s41598-021-86477-8.
50. Menniti FS, Knoth J, Diliberto EJ. Role of ascorbic acid in dopamine β-hydroxylation. The endogenous enzyme cofactor and putative electron donor for cofactor regeneration. J Biol Chem. 1986;261:16901–8. https://doi.org/10.1016/S0021-9258(19)75974-2.
51. May JM, Qu Z, chao, Nazarewicz R, Dikalov S. Ascorbic Acid Efficiently Enhances Neuronal Synthesis of Norepinephrine from Dopamine. Brain Res Bull. 2012;90:35. https://doi.org/10.1016/J.BRAINRESBULL.2012.09.009.
52. Ortega R, García N. The flavonoid quercetin induces changes in mitochondrial permeability by inhibiting adenine nucleotide translocase. J Bioenerg Biomembr. 2009;41:41–7. https://doi.org/10.1007/S10863-009-9198-6.
53. Li F, Li D, Yan X, Zhu F, Tang S, Liu J, et al. Quercetin Promotes the Repair of Mitochondrial Function in H9c2 Cells Through the miR-92a-3p/Mfn1 Axis. Curr Pharm Biotechnol. 2024;25:1858–66. https://doi.org/10.2174/0113892010266863231030052150.
54. Jin S-G, Meng Y, Johnson J, Szabó PE, Pfeifer GP. Concordance of hydrogen peroxide–induced 8-oxo-guanine patterns with two cancer mutation signatures of upper GI tract tumors. Sci Adv. 2022;8. https://doi.org/10.1126/sciadv.abn3815.
55. Federico A, Cardaioli E, Da Pozzo P, Formichi P, Gallus GN, Radi E. Mitochondria, oxidative stress and neurodegeneration. J Neurol Sci. 2012. https://doi.org/10.1016/j.jns.2012.05.030.
56. HAMAI D, BONDY SC. Oxidative Basis of Manganese Neurotoxicity. Ann N Y Acad Sci. 2004;1012:129–41. https://doi.org/10.1196/annals.1306.010.
57. Andersen JK. Oxidative stress in neurodegeneration: Cause or consequence? Nat Rev Neurosci. 2004. https://doi.org/10.1038/nrn1434.
58. Massie HR, Baird MB, Piekielniak MJ. Ascorbic acid and longevity in Drosophila. Exp Gerontol. 1976;11:37–41. https://doi.org/10.1016/0531-5565(76)90009-7.
59. Massie HR, Shumway ME, Whitney SJP, Sternick SM, Aiello VR. Ascorbic acid in Drosophila and changes during aging. Exp Gerontol. 1991;26:487–94. https://doi.org/10.1016/0531-5565(91)90037-M.
60. Omoboyowa DA, Olugbenga ST, Adetuyi FD, Akinsulure ST, Akinwande KM, Iwuji CB, et al. Modulatory effects of selected compounds on oxidative stress in hydrogen peroxide-induced Drosophila melanogaster. Pharmacol Res - Mod Chin Med. 2022;5:100169. https://doi.org/10.1016/j.prmcm.2022.100169.
61. Genç B, Karaman M. Effect of Ascorbic Acid on Oxidative Stress Parameters of Fruit Fly in the Presence of Fe (II). Biol Trace Elem Res. 2024;202:3810–5. https://doi.org/10.1007/s12011-023-03960-1.
62. Suh HJ, Shin B, Han S-H, Woo MJ, Hong K-B. Behavioral Changes and Survival in Drosophila melanogaster: Effects of Ascorbic Acid, Taurine, and Caffeine. Biol Pharm Bull. 2017;40:1873–82. https://doi.org/10.1248/bpb.b17-00321.
63. Proshkina E, Lashmanova E, Dobrovolskaya E, Zemskaya N, Kudryavtseva A, Shaposhnikov M, et al. Geroprotective and radioprotective activity of quercetin, (-)-epicatechin, and ibuprofen in Drosophila melanogaster. Front Pharmacol. 2016;7. https://doi.org/10.3389/fphar.2016.00505.
64. Nagpal I, Abraham SK. Ameliorative effects of gallic acid, quercetin, and limonene on urethane-induced genotoxicity and oxidative stress in Drosophila melanogaster. Toxicol Mech Methods. 2017;27:286–92. https://doi.org/10.1080/15376516.2016.1278294.
65. Zhao F, Cai T, Liu M, Zheng G, Luo W, Chen J. Manganese induces dopaminergic neurodegeneration via microglial activation in a rat model of manganism. Toxicol Sci. 2009. https://doi.org/10.1093/toxsci/kfn213.
66. Martin KV, Edmondson D, Cecil KM, Bezi C, Vance ML, McBride D, et al. Manganese Exposure and Neurologic Outcomes in Adult Populations. Neurol Clin. 2020;38:913–36. https://doi.org/10.1016/j.ncl.2020.07.008.
67. Hahm JY, Park J, Jang E-S, Chi SW. 8-Oxoguanine: from oxidative damage to epigenetic and epitranscriptional modification. Exp Mol Med. 2022;54:1626–42. https://doi.org/10.1038/s12276-022-00822-z.
68. Aschner M, Erikson KM, Dorman DC. Manganese Dosimetry: Species Differences and Implications for Neurotoxicity. Crit Rev Toxicol. 2005;35:1–32. https://doi.org/10.1080/10408440590905920.
69. Seong K-H, Uemura T, Kang S. Road to sexual maturity: Behavioral event schedule from eclosion to first mating in each sex of Drosophila melanogaster. iScience. 2023;26:107502. https://doi.org/10.1016/j.isci.2023.107502.

Publisher's note